Cancer Therapy: Preclinical

Clinical Cancer Research

Enhanced Cancer Immunotherapy by Chimeric Antigen Receptor–Modified T Cells Engineered to Secrete Checkpoint Inhibitors

Si Li[1], Natnaree Siriwon[2], Xiaoyang Zhang[2], Shuai Yang[3], Tao Jin[4], Feng He[4], Yu Jeong Kim[1], John Mac[2], Zhengfei Lu[5,6,7,8], Sijie Wang[9], Xiaolu Han[10], and Pin Wang[1,2,11]

Abstract

Purpose: Despite favorable responses of chimeric antigen receptor (CAR)-engineered T-cell therapy in patients with hematologic malignancies, the outcome has been far from satisfactory in the treatment of solid tumors, partially owing to the development of an immunosuppressive tumor microenvironment. To overcome this limitation, we engineered CAR T cells secreting checkpoint inhibitors (CPI) targeting PD-1 (CAR.αPD1-T) and evaluated their efficacy in a human lung carcinoma xenograft mouse model.

Experimental Design: To evaluate the effector function and expansion capacity of CAR.αPD1-T cells *in vitro*, we measured the production of IFNγ and T-cell proliferation following antigen-specific stimulation. Furthermore, the antitumor efficacy of CAR.αPD1-T cells, CAR T cells, and CAR T cells combined with anti–PD-1 antibody was determined using a xenograft mouse model. Finally, the underlying mechanism was investigated by analyzing the expansion and functional capacity of TILs.

Results: Human anti–PD-1 CPIs secreted by CAR.αPD1-T cells efficiently bound to PD-1 and reversed the inhibitory effect of PD-1/PD-L1 interaction on T-cell function. PD-1 blockade by continuously secreted anti–PD-1 attenuated the inhibitory T-cell signaling and enhanced T-cell expansion and effector function both *in vitro* and *in vivo*. In the xenograft mouse model, we demonstrated that the secretion of anti–PD-1 enhanced the antitumor activity of CAR T cells and prolonged overall survival.

Conclusions: With constitutive anti–PD-1 secretion, CAR.α PD1-T cells are more functional and expandable, and more efficient at tumor eradication than parental CAR T cells. Collectively, our study presents an important and novel strategy that enables CAR T cells to achieve better antitumor immunity, especially in the treatment of solid tumors. *Clin Cancer Res; 23(22); 6982–92. ©2017 AACR.*

Introduction

Adoptive cell transfer (ACT), as a modality of immunotherapy for cancer, has demonstrated remarkable success in treating hematologic malignancies and malignant melanoma (1–5). An especially effective form of ACT, which uses gene-modified T cells expressing a chimeric antigen receptor (CAR) to specifically target tumor-associated antigen (TAA), such as CD19 and GD2, has displayed encouraging results in clinical trials for treating such diseases as B-cell malignancies and neuroblastoma (6–8).

Unlike naturally occurring T-cell receptors (TCR), CARs are artificial receptors consisting of an extracellular antigen recognition domain fused with intracellular T-cell signaling and costimulatory domains. CARs can directly and selectively recognize cell surface TAAs in an MHC-independent manner (9). Despite the documented success of CAR T-cell therapy in patients with hematologic malignancies, only modest responses have been observed in solid tumors. This can be attributed, in part, to the establishment of an immunosuppressive microenvironment in solid tumors. Such milieu involves the upregulation of a number of intrinsic inhibitory pathways mediated by increased expression of inhibitory receptors (IR) in T cells reacting with their cognate ligands within the tumor (10, 11).

So far, several IRs have been characterized in T cells, such as cytotoxic T-lymphocyte–associated protein 4 (CTLA-4), T-cell immunoglobulin domain and mucin domain–containing protein 3 (TIM-3; also known as HAVCR2), lymphocyte-activation gene 3 (LAG-3), and programmed death-1 (PD-1; ref. 12). These

[1]Department of Pharmacology and Pharmaceutical Sciences, University of Southern California, Los Angeles, California. [2]Mork Family Department of Chemical Engineering and Materials Sciences, University of Southern California, Los Angeles, California. [3]Department of Biochemistry and Molecular Biology, University of Southern California, Los Angeles, California. [4]Technology Department, HRAIN Biotechnology Co., Ltd., Shanghai, China. [5]Department of Pathology, University of Southern California Keck School of Medicine, Norris Comprehensive Cancer Center, Los Angeles, California. [6]Department of Biochemistry and Molecular Biology, University of Southern California Keck School of Medicine, Norris Comprehensive Cancer Center, Los Angeles, California. [7]Department of Biological Sciences, University of Southern California Keck School of Medicine, Norris Comprehensive Cancer Center, Los Angeles, California. [8]Department of Molecular Microbiology and Immunology, University of Southern California Keck School of Medicine, Norris Comprehensive Cancer Center, Los Angeles, California. [9]Department of Medicinal Chemistry and Molecular Pharmacology, Purdue University, West Lafayette, Indiana. [10]Genetic, Molecular and Cellular Biology Program, Keck School of Medicine, University of Southern California, Los Angeles, California. [11]Department of Biomedical Engineering, University of Southern California, Los Angeles, California.

Note: Supplementary data for this article are available at Clinical Cancer Research Online (http://clincancerres.aacrjournals.org/).

S. Li and N. Siriwon contributed equally to this article.

Corresponding Author: Pin Wang, University of Southern California, 3710 McClintock Avenue, RTH506, Los Angeles, CA 90089. Phone: 213-740-0780; Fax: 213-740-8053; E-mail: pinwang@usc.edu

doi: 10.1158/1078-0432.CCR-17-0867

Translational Relevance

Chimeric antigen receptor (CAR) T cells with antitumor activity are frequently compromised in the immunosuppressive tumor microenvironment. The PD-1 receptor is one of the major effector molecules in mediating inhibitory T-cell signaling. A previous study demonstrated that anti–PD-1 antibody treatment enhanced antitumor activity when combined with anti-HER2 CAR T cells in a syngeneic breast carcinoma mouse model. However, achieving a substantial and sustained efficacy requires continuous administration and a large amount of antibodies, often leading to severe systemic toxicity. Therefore, instead of administering the anti–PD-1 antibody systemically, we engineered anti–PD-1 self-secreting CAR.α PD1-T cells, which are more functional and expandable, and more efficient at mediating tumor eradication compared with injection of CAR T cells alone, or the combined injection of anti–PD-1 antibody with the CAR T cells. Our study provides an efficient and safe strategy for combining CPI treatment with CAR T-cell therapy for immunotherapy in solid tumors.

molecules are upregulated following sustained activation of T cells in chronic disease and cancer, and they promote T-cell dysfunction and exhaustion, thus resulting in the escape of tumor from immunosurveillance (12). Unlike other IRs, PD-1 is upregulated shortly after T-cell activation, which, in turn, inhibits T-cell effector function via interacting with its two ligands, PD-L1 or PD-L2. PD-L1 is constitutively expressed on T cells, B cells, macrophages, and dendritic cells (DC; ref. 13). PD-L1 is also shown to be abundantly expressed in a wide variety of solid tumors (14–16). In contrast, the expression of PD-L1 in normal tissues is undetectable (15). As a consequence of its critical role in immunosuppression, PD-1 has been the focus of recent research, aiming to neutralize its negative effect on T cells and enhance antitumor responses. Clinical studies have demonstrated that PD-1 blockade significantly enhanced tumor regression in colon, renal and lung cancers, and melanoma (12).

A recent study shows tumor-induced hypofunction of CAR T cells as well as upregulation of PD-1 on the CAR T cells and demonstrates the contribution of PD-1 to the dysfunction of tumor-infiltrating CAR T cells (17), thereby suggesting a potential strategy whereby CAR T therapy could be combined with PD-1 blockade in cancer treatment (18). Therefore, in this study, to overcome the inhibitory effect of PD-1 signaling in CAR T cells, we genetically engineered CAR T cells with the capacity to constitutively produce a single-chain variable fragment (scFv) form of anti–PD-1 antibody. In our own tumor models, we found that anti–PD-1 scFv expression and secretion could interrupt the engagement of PD-1 with its ligand, PD-L1, and prevent CAR T cells from being inhibited and exhausted. Most importantly, in a CD19 tumor model, we demonstrated for the first time that the secretion of anti–PD-1 scFv by CAR T cells could significantly improve the capacity of CAR T cells in eradicating an established solid tumor.

Materials and Methods

General methods for cell culture, supplementary reagents, antibodies, ELISA assay, specific cell lysis assay, cell proliferation assay, and Western blotting analysis are detailed in the electronic Supplementary Material. Detailed information about retroviral vector production, T-cell transduction and expansion, surface immunostaining analysis, and intracellular cytokine staining analysis is provided in our previous publication (19).

Mice

Six- to 8-week-old female NOD.Cg-*Prkdc*^{scid} *Il2rg*^{tm1Wjl}/SzJ (NSG) mice were purchased from The Jackson Laboratory. All animal studies were performed in accordance with the Animal Care and Use Committee guidelines of the NIH (Bethesda, MD) and were conducted under protocols approved by the Animal Care and Use Committee of the USC.

Cell lines

Cell lines SKOV3 and 293T were obtained directly from ATCC for this study. The lung cancer line NCI-H292 was kindly provided by Dr. Ite Laird-Offringa (University of Southern California, Los Angeles, CA) and was used without further authentication. The H292-CD19 and SKOV3-CD19 cell lines were generated by the transduction of parental NCI-H292 and SKOV3 cells with a lentiviral vector encoding the cDNA of human CD19. All cells were routinely tested for potential mycoplasma contamination using the MycoSensor qPCR Assay Kit (Agilent Technologies).

Plasmid construction

The retroviral vector encoding anti-CD19 CAR (CAR) was constructed on the basis of the MP71 retroviral vector kindly provided by Prof. Wolfgang Uckert, as described previously (20). The vector encoding anti-CD19 CAR with anti–PD-1 scFv (CAR.α PD1) was then generated on the basis of the anti-CD19 CAR. The insert for CAR.αPD1 vector consisted of the following components in frame 5′ end to 3′ end: a NotI site, the anti-CD19 CAR, a leader sequence derived from human IL2, the anti-PD-1 scFv light chain variable region, a GS linker, the anti–PD-1 scFv heavy chain variable region, the HA-tag sequence, and an EcoRI site.

The anti–PD-1 scFv portion in the CAR.αPD1 vector was derived from the amino acid sequence of human mAb 5C4 specific against human PD-1 (21). The corresponding DNA sequence of the scFv was codon optimized for its optimal expression in human cells using the online codon optimization tool and was synthesized by Integrated DNA Technologies. The anti-PD-1 scFv was then ligated into the CD19 CAR vector via the EcoRI site through the Gibson assembly method.

Competitive blocking assay

The 96-well assay plates (Thermo Fisher Scientific) were coated with 3 μg/mL of anti-human CD3 antibody at 4°C overnight. On the second day, the supernatant of the wells was aspirated, and the wells were washed once with 100 μL per well of PBS. rhPD-L1/Fc (10 μg/mL; R&D Systems) in 100 μL of PBS was added. In each well, 100 μg/mL of goat anti-human IgG Fc antibody in 10 μL of PBS was then added. The assay plate was incubated for 4 hours at 37°C. Human T cells were harvested, washed once, and then resuspended to 1×10^6 cells/mL in TCM. The wells of the assay plate were aspirated. Then, 100 μL of human T-cell suspension (1×10^5) and 100 μL of supernatant of CAR or CAR.αPD1 T-cell culture 3-day posttransduction, supplemented with GolgiPlug (BD Biosciences), were added to each well. The plate was covered and incubated at 37°C and 5% CO_2 overnight. After incubation, T cells were harvested and stained with IFNγ intracellularly.

Tumor model and adoptive transfer

At 6 to 8 weeks of age, mice were inoculated subcutaneously with 3×10^6 H292-CD19 cells, and 10 to 13 days later, when the average tumor size reached 100 to 120 mm^3, mice were treated with intravenous adoptive transfer of 1×10^6 or 3×10^6 CAR-transduced T cells in 100 μL PBS. CAR expression was normalized to 20% in both CAR groups by addition of donor-matched nontransduced T cells. Tumor growth was monitored twice a week. Tumor size was measured by calipers and calculated by the following formula: $W^2 \times L/2$. Mice were euthanized when they displayed obvious weight loss, ulceration of tumors, or tumor size larger than 1,000 mm^3. For PD-1 blockade, tumor-bearing mice were injected intraperitoneally with 125 μg anti-human PD-1 mAb (J116; Bio X Cell) twice a week for 2 weeks.

Statistical analysis

Statistical analysis was performed in GraphPad Prism, version 5.01. One-way ANOVA with Tukey multiple comparison was performed to assess the differences among different groups in the *in vitro* assays. Tumor growth curve was analyzed using one-way ANOVA with repeated measures (Tukey multiple comparison method). Mouse survival curve was evaluated by the Kaplan–Meier analysis (log-rank test with Bonferroni correction). A $P < 0.05$ was considered statistically significant. Significance of findings was defined as: ns = not significant, $P > 0.05$; *, $P < 0.05$; **, $P < 0.01$; ***, $P < 0.001$.

Results

Characterization of anti-CD19 CAR T cells secreting anti–PD-1 antibody

The schematic representation of the retroviral vector constructs used in this study is shown in Fig. 1A. The retroviral vector encoding the anti-CD19 CAR composed of anti-CD19 scFv, CD8 hinge, CD28 transmembrane, and intracellular costimulatory domains, as well as intracellular CD3ζ domain was designated as CAR19. The retroviral vector encoding both anti-CD19 CAR and secreting anti-PD-1 scFv was designated as CAR19.αPD1. Human PBMCs were transduced with each construct to test the expression of CAR in primary lymphocytes. As seen in Fig. 1B, CAR expression was observed for both constructs in human T cells, although anti–PD-1–secreting CAR19 T cells expressed slightly lower level of the CAR on the cell surface. Expression and secretion of anti–PD-1 was assessed by performing Western blotting analysis and ELISA on the cell supernatant 3 days after transduction. We observed that anti–PD-1 could be successfully expressed and secreted by T cells transduced with CAR19.αPD1 (Fig. 1C and D). Furthermore, to better quantify the amount of anti–PD-1 secreted by CAR19.αPD1 T cells, we seeded 1×10^6 of CAR19.αPD1 T cells and cultured for 24 hours with or without brefeldin A. The anti–PD-1 scFv in the cell culture supernatant was then measured by ELISA. Approximately 0.1 μg/mL of anti–PD-1 was present in the supernatant (Supplementary Fig. S1A). The expression of anti–PD-1 scFv was also monitored over the course of CAR19.αPD1 T-cell expansion. We found that the production of anti–PD-1 was maintained at a relatively stable level (0.2–0.5 μg/mL; Supplementary Fig. S1B).

To evaluate the binding activity of anti–PD-1 scFv secreted by CAR19.αPD1 T cells, we incubated the activated T cells with CAR19.αPD1 T-cell culture supernatant for 30 minutes. The T cells were then stained with anti-HA antibody to detect the bound anti–PD-1 on the T-cell surface. Compared with the control medium incubation, the secreted anti–PD-1 was able to bind to the PD-1 on the activated T-cell surface and then detected by the anti-HA antibody (Supplementary Fig. S1C and S1D). To further investigate the blocking function of anti–PD-1 scFv secreted by CAR19.αPD1 T cells, a competitive binding and blocking assay was performed. Intracellular IFNγ was measured to assess the activity of the T cells. As shown in Fig. 1E, the expression of IFNγ was upregulated when the T cells were stimulated by anti-CD3 antibody, and indeed, the presence of recombinant human PD-L1 (rhPD-L1) resulted in significantly lower IFNγ expression. However, adding the cell culture supernatant from CAR19.αPD1 T cells effectively reversed the inhibitory effect of rhPD-L1 on the T cells and significantly increased IFNγ production (Fig. 1E).

Secreting anti–PD-1 antibody enhances the antigen-specific immune responses of CAR T cells

To further assess the effector function of anti–PD-1–secreting CAR19 T cells through antigen-specific stimulation, both CAR19 and CAR19.αPD1 T cells were cocultured for different durations with H292-CD19 or SKOV3-CD19 target cells, both of which were shown to have high surface expression of PD-L1 (Supplementary Fig. S2A). T cells at different time points were then harvested, and the cell function marker IFNγ in the supernatant was measured by ELISA. Upon antigen stimulation for 24 hours, we found that both CAR19 and CAR19.αPD1 T cells had a similar amount of IFNγ secretion (Fig. 2A; Supplementary Fig. S2B and S2C). However, after 72 hours of stimulation with H292-CD19 cells, CAR19.αPD1 T cells secreted significantly higher IFNγ compared with the parental CAR19 T cells (Fig. 2A; Supplementary Fig. S2C). Combination of CAR19 T cells with anti–PD-1 antibody (0.6 μg/mL) resulted in IFNγ expression comparable with the parental CAR19 T cells after stimulation (Supplementary Fig. S2C). Similarly, after 96 hours of antigen stimulation, CAR19 T cells secreting anti–PD-1 expressed significantly more IFNγ than that expressed by the parental CAR19 T cells (Fig. 2A; Supplementary Fig. S2B).

Next, the cytolytic function of engineered T cells was examined by a 6-hour cytotoxicity assay. The cytotoxic activity of CAR19 and CAR19.αPD1 T cells against H292-CD19 cells was evaluated at effector/target (E/T) ratios of 1, 5, 10, and 20. We found that both CAR19 and CAR19.αPD1 T cells mediated significant target cell lysis, especially at higher E/T ratios in comparison with the nontransduced T cells. However, little difference was found between CAR19 and CAR19.αPD1 T cells in terms of cytolytic activity (Fig. 2B).

T-cell proliferation was then evaluated by a carboxyfluorescein diacetate succinimidyl ester (CFSE)-based proliferation assay after 96-hour coculture of engineered T cells with target H292-CD19 cells. We observed that antigen-specific stimulation of both CAR19 and CAR19.αPD1 T cells resulted in a markedly higher level of proliferation rate compared with nontransduced T cells. Moreover, compared with CAR19 T cells (57.9% ± 10.2%), the proliferation rate of CAR19.αPD1 T cells (75.9% ± 5.5%) was significantly higher (Fig. 2C and D). The cell proliferation potential was further assessed by cell expansion. With antigen-specific stimulation, it was shown that both CAR19 and CAR19.αPD1 T cells significantly expanded compared with the nontransduced T cells. Remarkably, in comparison with parental CAR19 T cells (2.4 ± 0.2), the number of cell doublings was significantly higher in CAR19.αPD1 T cells (3.2 ± 0.3; Supplementary Fig. S3).

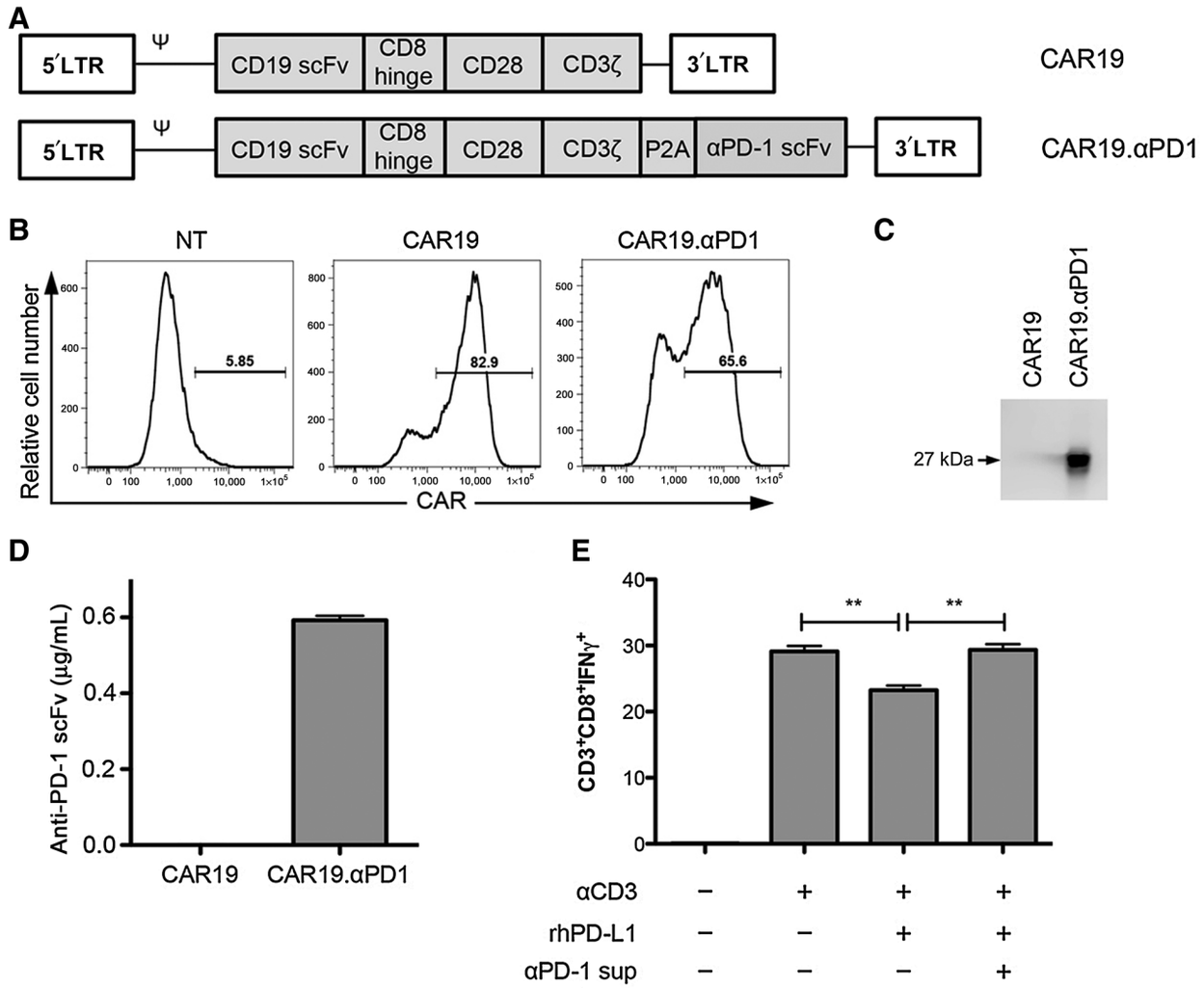

Figure 1.

Construction and characterization of CAR19 and CAR19.αPD1. **A,** Schematic representation of parental anti-CD19 CAR (CAR19) and anti–PD-1–secreting anti-CD19 CAR (CAR19.αPD1) constructs. **B,** Expression of both CARs in human T cells. The two groups of CAR T cells were stained with biotinylated protein L followed by FITC-conjugated streptavidin to detect CAR expression on the cell surface. A viable $CD3^+$ lymphocyte gating strategy was used. NT indicates nontransduced T cells, which were used as a control. **C** and **D,** Expression of secreted anti–PD-1 antibody in the supernatant from either CAR19 or CAR19.αPD1 T-cell culture was analyzed by Western blot (**C**) and ELISA (**D**). **E,** The percentage of $CD8^+$ T cells expressing IFNγ over total $CD8^+$ T cells with the indicated treatment ($n = 4$, mean ± SEM; **, $P < 0.01$).

Secreting anti–PD-1 limits the upregulation of PD-1 on CAR T cells after antigen stimulation

To assess the effect of secreted anti–PD-1 scFv on protecting human T cells from functional inhibition, the engineered CAR T cells were cocultured with either H292-CD19 or SKOV3-CD19 target cells for 24 hours and then stained for the T-cell–inhibitory marker PD-1. We found that the expression of PD-1 was significantly upregulated in both CAR19 and CAR19.αPD1 T cells following antigen-specific stimulation. In comparison, the upregulated PD-1 expression on CAR19.αPD1 T cells was significantly lower than that on parental CAR19 T cells (Fig. 3A and B; Supplementary Fig. S6A). However, without antigen-specific stimulation, the expression of PD-1 in both CAR19 and CAR19.αPD1 T cells maintained at a similar and stable level over the course of T-cell expansion (Supplementary Fig. S6B).

To further determine whether the lower expression of PD-1 in CAR19.αPD1 T cells is due to the blocking function of secreted anti–PD-1 scFv on the binding of PD-1 detection antibody or the downregulation of PD-1, we incubated the activated T cells with either the control medium or CAR19.α PD1 T-cell culture supernatant for 30 minutes before staining them with anti–PD-1 antibody. We found that the secreted anti–PD-1 scFv was able to block approximately 20% of the binding of the PD-1 detection antibody (Supplementary Fig. S4A). In tandem, we cocultured either the CAR19 or CAR19.αPD1 T cells with target cells H292-CD19 for 24 hours. Both T cells were then harvested and the transcriptional expression of PD-1 was measured by qPCR. We observed that PD-1 expression in CAR19.αPD1 T cells was significantly lower than that in parental CAR19 T cells (Supplementary Fig. S4B). This

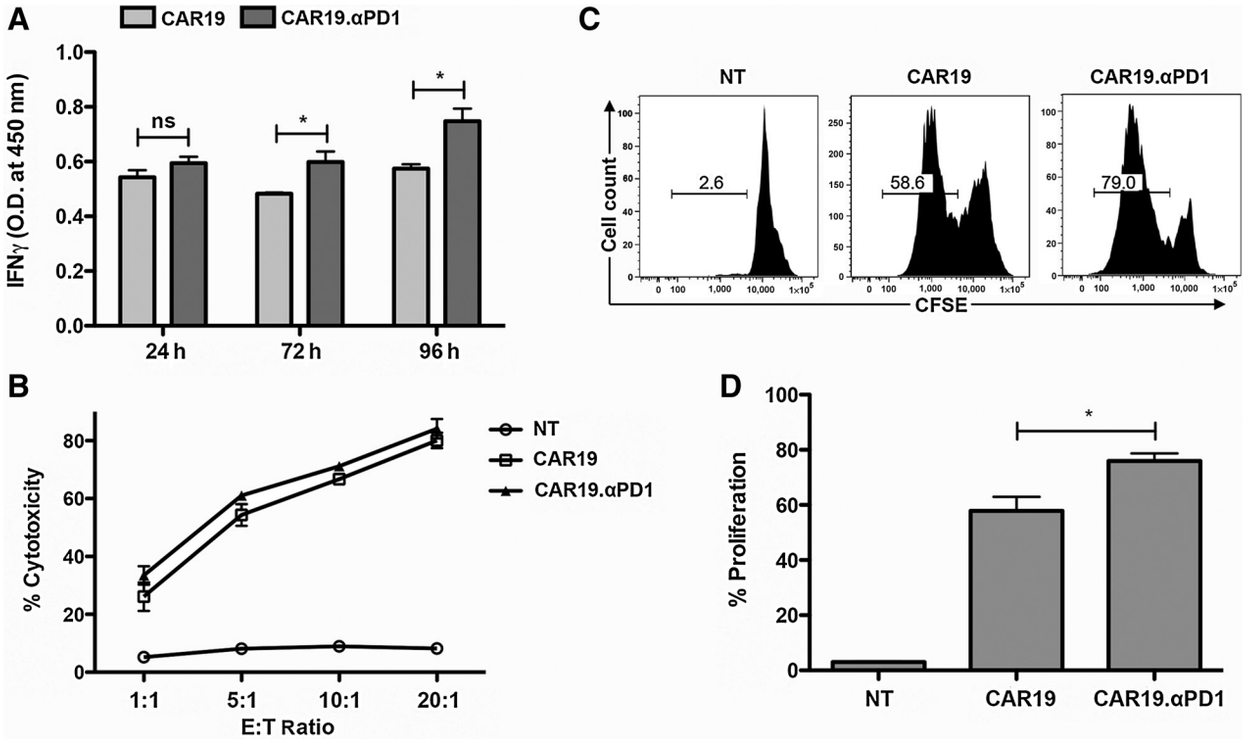

Figure 2.

Anti–PD-1 expression enhanced the antigen-specific immune responses of CAR T cells. **A,** Both CAR19 and CAR19.αPD1 T cells were cocultured with H292-CD19 cells for different durations. IFNγ production was measured by ELISA ($n = 5$, mean ± SEM; ns, not significant, $P > 0.05$; *, $P < 0.05$). **B,** Cytotoxicity of both CARs against target cells. The two groups of CAR T cells were cocultured for 6 hours with H292-CD19 cells at 1:1, 5:1, 10:1, and 20:1 effector-to-target ratios, and cytotoxicity against H292-CD19 was measured. Nontransduced (NT) T cells were used as a control. **C,** Proliferation of both CARs after antigen-specific stimulation. The two groups of CAR T cells were prestained with CFSE. The stained T cells were then cocultured for 96 hours with H292-CD19 cells at 1:1 effector-to-target ratio, and the intensity of CFSE was measured. Nontransduced (NT) T cells were used as a control. **D,** The summarized statistics of proliferation rate for nontransduced (NT) T cells, CAR19 T cells, and CAR19.αPD1 T cells in **C** were shown in bar graphs ($n = 4$, mean ± SEM; *, $P < 0.05$).

indeed confirms that CAR19.αPD1 T cells have downregulated PD-1 expression.

In addition to PD-1, other cell surface–inhibitory molecules, including LAG-3, TIM-3, and CTLA-4, also play important roles in inducing inhibitory signals and limiting the antitumor efficacy of CAR T-cell therapy (12). To evaluate whether the expression of other T-cell–inhibitory markers is regulated by CAR stimulation, we measured the expression of LAG-3 and TIM-3 on CAR-engineered T cells. Similar to PD-1, we found that the expression of LAG-3 and TIM-3 was significantly upregulated on both CAR19 and CAR19.αPD1 T cells following antigen stimulation, compared with nontransduced T cells. In comparison with CAR19 T cells, CAR19.αPD1 T cells expressed slightly lower LAG-3 and TIM-3 after stimulation with H292-CD19 cells. Moreover, upon SKOV3-CD19 stimulation, CAR19.αPD1 T cells had significantly lower LAG-3 expression than CAR19 T cells, whereas they had similar TIM-3 expression (Fig. 3C and D; Supplementary Figs. S5A and S6A). In comparison, without antigen-specific stimulation, LAG-3 in CAR19 and CAR19.αPD1 T cells was expressed at a similar level and remained stable over the course of T-cell expansion (Supplementary Fig. S6B).

It has been shown that PD-1 blockade could promote the survival of GD2 CAR T cells after activation with the PD-L1–negative target cells, indicating that the interaction between PD-1–expressing T cells and T cells expressing PD-1 ligands, such as PD-L1, might contribute to the suppression of T-cell function (22). Thus, in this experiment, we also measured the expression of PD-L1 in both CAR19 and CAR19.αPD1 T cells and found that it was significantly increased following antigen-specific stimulation. However, the expression of PD-L1 in CAR19.αPD1 T cells was significantly lower than that in CAR19 T cells (Fig. 3E; Supplementary Fig. S5B).

Anti–PD-1 engineered CAR T cells exhibit enhanced antitumor reactivity

To evaluate the antitumor efficacy of CAR19.αPD1 T cells, we adoptively transferred 1×10^6 CAR-engineered T cells into NSG mice bearing established H292-CD19 subcutaneous tumors (~100 mm^3). The experimental procedure for animal study is shown in Fig. 4A. The data in Fig. 4B demonstrate that all three anti-CD19 CAR T-cell groups showed decreased tumor sizes compared with nontransduced T cells or nontransduced T cells combined with anti–PD-1 antibody treatment over the course of the experiment. However, in comparison with parental CAR19 T cells or CAR19 T cells combined with anti–PD-1 antibody treatment, CAR19.αPD1 T-cell treatment significantly enhanced the antitumor effect, which became evident as early as one week after T-cell infusion (Fig. 4B). Notably, 17 days after adoptive cell

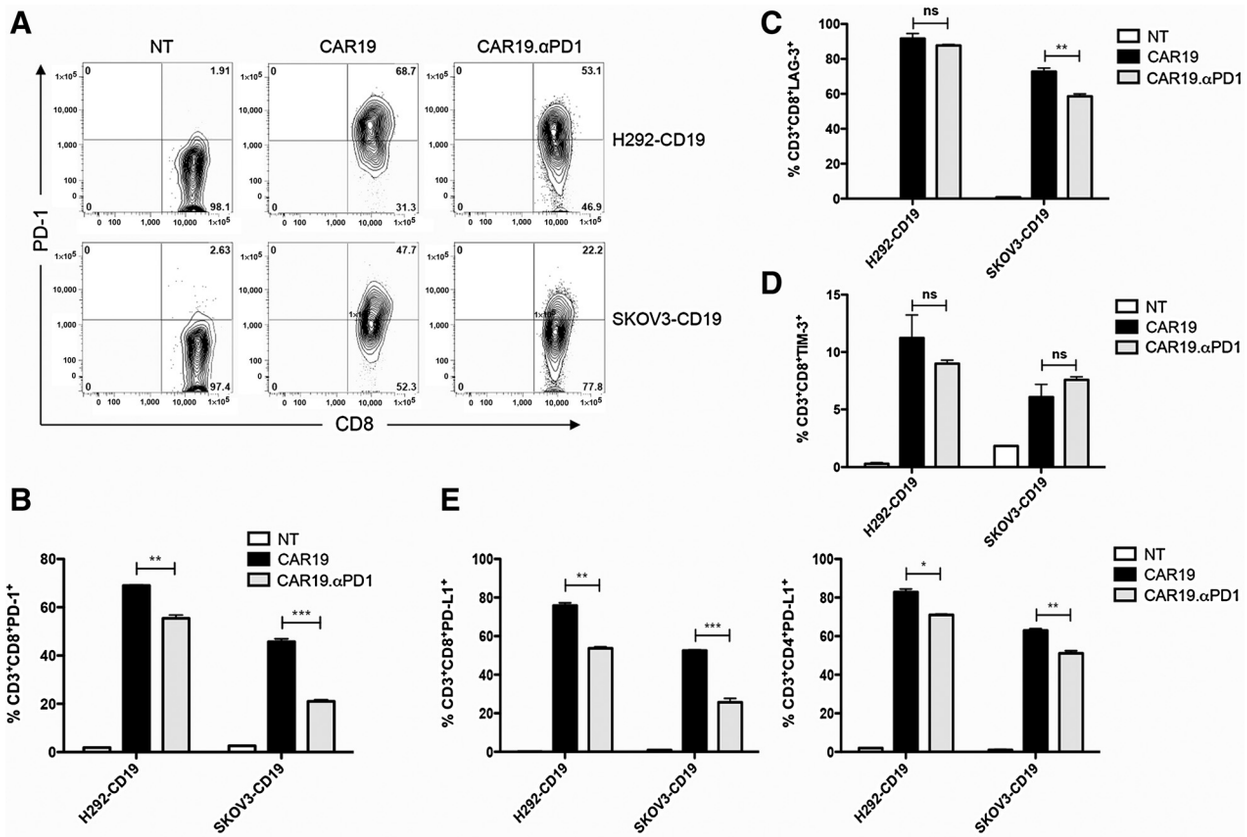

Figure 3.

Secreting anti–PD-1 scFv protected CAR T cells from being exhausted. Both CAR19 and CAR19.αPD1 T cells were cocultured with either H292-CD19 or SKOV3-CD19 cells for 24 hours. **A,** PD-1 expression was measured by flow cytometry. $CD8^+$ T cells were shown in each panel. PD-1–expressing CD8 T cells were gated, and their percentage over total $CD8^+$ T cells was shown in each scatterplot. **B,** The summarized statistics of triplicates were shown in bar graphs ($n = 3$, mean ± SEM; **, $P < 0.01$; ***, $P < 0.001$). **C,** LAG-3 expression was measured by flow cytometry. The percentage of LAG-3–expressing CD8 T cells over total $CD8^+$ T cells was shown in bar graphs ($n = 3$, mean ± SEM; ns, not significant, $P > 0.05$; **, $P < 0.01$). **D,** TIM-3 expression was measured by flow cytometry. The percentage of TIM-3–expressing CD8 T cells over total $CD8^+$ T cells was shown in bar graphs ($n = 3$, mean ± SEM; ns, not significant, $P > 0.05$). **E,** Both CAR19 and CAR19.αPD1 T cells were cocultured with either H292-CD19 or SKOV3-CD19 cells for 24 hours. PD-L1 expression was measured by flow cytometry. The percentages of PD-L1–expressing CD8 T cells over total $CD8^+$ T cells and PD-L1–expressing CD4 T cells over total $CD4^+$ T cells were shown in bar graphs ($n = 3$, mean ± SEM; *, $P < 0.05$; **, $P < 0.01$; ***, $P < 0.001$).

transfer, we observed that the tumors from mice treated with CAR19.αPD1 T cells almost disappeared. In the parental CAR19 T-cell group or combination group, 4 of 6 mice (~70%) still had either progressive or stable disease states and only experienced a decrease in tumor size of less than 30% (Fig. 4C). The overall survival of the tumor-bearing mice was also evaluated. It showed that CAR19.αPD1 T-cell treatment significantly prolonged long-term survival (100%), compared with either the parental CAR19 T-cell treatment alone (17%) or the combined anti–PD-1 antibody and CAR19 T-cell treatment (17%; Fig. 4D).

Anti–PD-1 engineered CAR T cells can expand more *in vivo* than parental CAR T cells

Next, the engraftment and expansion of CAR T cells were assessed *in vivo*. Two days following T-cell infusion, mice were euthanized, and different organs and tissues, including the tumor, blood, spleen, and bone marrow, were harvested for human T-cell staining. We found that T-cells in all groups had barely expanded and that less than 2% of T cells could be observed in all examined tissues. Most T cells (1%–2%) homed to the spleen, while a certain percentage of T cells (0.1%–0.5%) circulated were in the blood. The infiltration level of transferred T cells was low in tumor and bone marrow. In addition, the T-cell percentage between the nontransduced and CAR-transduced T cells showed little difference across all examined tissues (Fig. 5A). However, one week after T-cell infusion, on day 10, we observed a significant expansion of CAR T cells in all examined tissues, whereas nontransduced T cells were barely present. Notably, consistent with our *in vitro* data, CAR19.αPD1 T cells had a significantly higher expansion rate compared with parental CAR19 T cells, especially in tumor, spleen, and blood (Fig. 5B and C).

Anti–PD-1 engineered CAR T cells lead to higher T-cell effector function at the established tumor site

To further determine whether the enhanced antitumor effects observed following CAR19.αPD1 T-cell therapy are correlated with increased function of CAR T cells at the tumor site, mice were

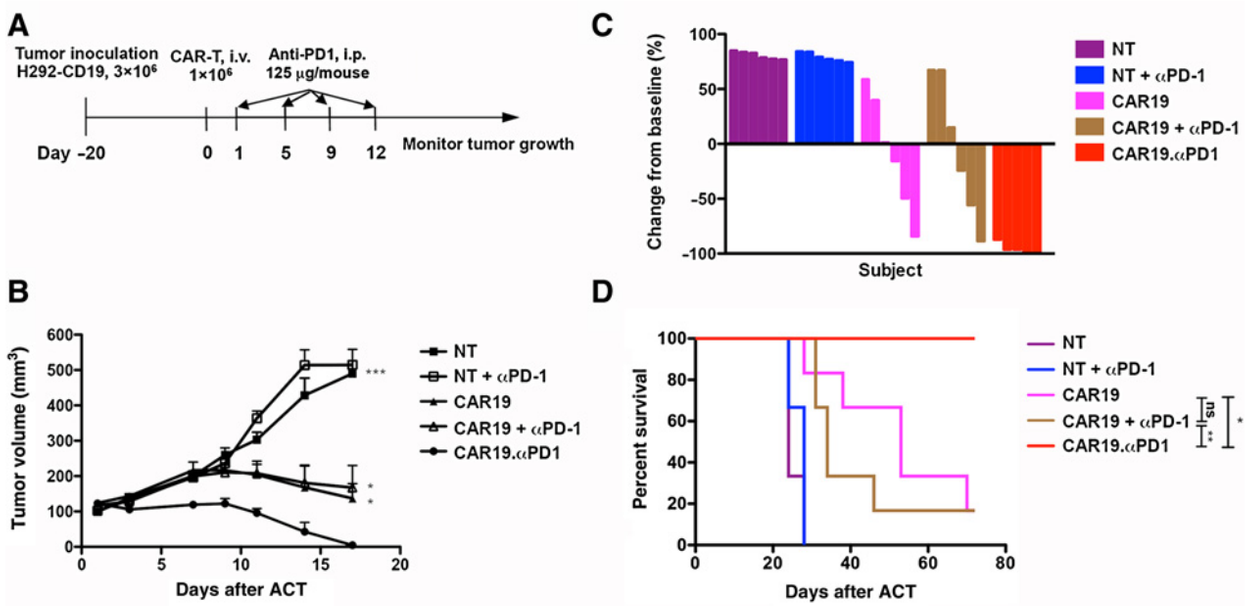

Figure 4.

Adoptive transfer of CAR T cells secreting anti–PD-1 scFv enhanced the growth inhibition of established tumor. **A,** Schematic representation of the experimental procedure for tumor challenge, T-cell adoptive transfer, and antibody treatment. NSG mice were subcutaneously challenged with 3×10^6 of H292-CD19 tumor cells. At day 20, when the tumors grew to approximately 100 mm^3, 1×10^6 of CAR19 or CAR19.αPD1 T cells were adoptively transferred through intravenous injection. One day after T-cell infusion, anti–PD-L1 antibody treatment was initiated, and the treatment was continued on the indicated dates. Tumor volume was measured every other day. **B,** Tumor growth curve for mice treated with nontransduced (NT), NT plus anti–PD-1 injection, CAR19, CAR19 plus anti–PD-1 injection, or CAR19.αPD1. Data were presented as mean tumor volume ± SEM at indicated time points ($n = 8$; *, $P < 0.05$; ***, $P < 0.001$). **C,** Waterfall plot analysis of tumor reduction on day 17 after therapy for various treatment groups. **D,** Survival of H292-CD19 tumor-bearing NSG mice after indicated treatment. Overall survival curves were plotted using the Kaplan–Meier method and compared using the log-rank (Mantel–Cox) test ($n = 6$; ns, not significant, $P > 0.05$; *, $P < 0.05$; **, $P < 0.01$).

challenged with H292-CD19 tumors before receiving 3×10^6 CAR T cells. The experimental design is shown in Fig. 6A. Eight days after T-cell infusion, we euthanized the mice and analyzed T cells in tumor, blood, spleen, and bone marrow, using flow cytometry. Compared with the CAR T-cell treatment, we observed that the injected anti–PD-1 antibody had little effect on enhancing the expansion of T cells *in vivo*. However, consistent with our previous observation (Fig. 5B), T cells from mice treated with the CAR19.αPD1 regimen expanded at a higher rate in tumor, blood, and spleen (Fig. 6B). It has been shown that the population of cytotoxic $CD8^+$ T cells among tumor-infiltrating lymphocytes (TIL) is critical in eliciting antitumor immunity and spontaneous tumor control (23). Therefore, the ratio of $CD8^+$ versus $CD4^+$ T cells was analyzed among TILs. Compared with the parental CAR19 T cells, results showed that the CAR19.αPD1 T cells had a significantly higher ratio of $CD8^+$ versus $CD4^+$ T cells, whereas the combination therapy had a similar $CD8^+$ versus $CD4^+$ T-cell ratio compared with CAR T-cell monotherapy (Fig. 6C). Similarly, in the blood and spleen, the ratio of $CD8^+$ versus $CD4^+$ in CAR19.αPD1 T-cell treatment was also significantly higher than that in parental CAR19 T-cell monotherapy and combination treatment groups (Fig. 6C), although there was little difference between the $CD8^+$ versus $CD4^+$ T-cell ratio between CAR19 and CAR19.αPD1 T cells before T-cell infusion (Supplementary Fig. S7A). Furthermore, we assessed PD-1 expression on tumor-infiltrating $CD8^+$ T cells and found that both the injected and secreted anti–PD-1 antibodies could significantly decrease the expression of PD-1 (Fig. 6D). We also performed the *ex vivo* culture and activated TILs with either anti-CD3/CD28 antibodies or target cell H292-CD19. We observed significantly higher expression of IFNγ in adoptively transferred CAR19.αPD1 T cells, compared with either parental CAR19 T cells or CAR19 T cells combined with systemic anti–PD-1 antibody treatment. Little difference was observed in IFNγ expression between CAR T-cell monotherapy and combined therapy (Fig. 6E and F). In addition, we measured the expression of IFNγ and anti–PD-1 antibodies in the sera and found little difference in IFNγ expression among all groups (Supplementary Fig. S7C). Notably, compared with CAR19 T-cell treatment, CAR19.αPD1 T-cell therapy had significantly higher anti–PD-1 concentration in the sera, although the concentration was more than 15-fold lower than that with systemic anti–PD-1 antibody injection (Fig. 6G).

Discussion

In this study, we engineered human anti-CD19 CAR T cells that secrete human anti–PD-1 scFvs and demonstrated that anti–PD-1 scFv could be efficiently expressed and secreted by CAR19.αPD1 T cells. The secreted scFvs successfully bound to PD-1 on the cell surface and reversed the inhibitory effects of PD-1/PD-L1 interaction on T-cell function. PD-1 blockade by constitutively secreted anti–PD-1 scFv decreased the inhibitory signal and significantly enhanced T-cell proliferation and effector function *in vitro*. Our study using xenograft mouse models also demonstrated that

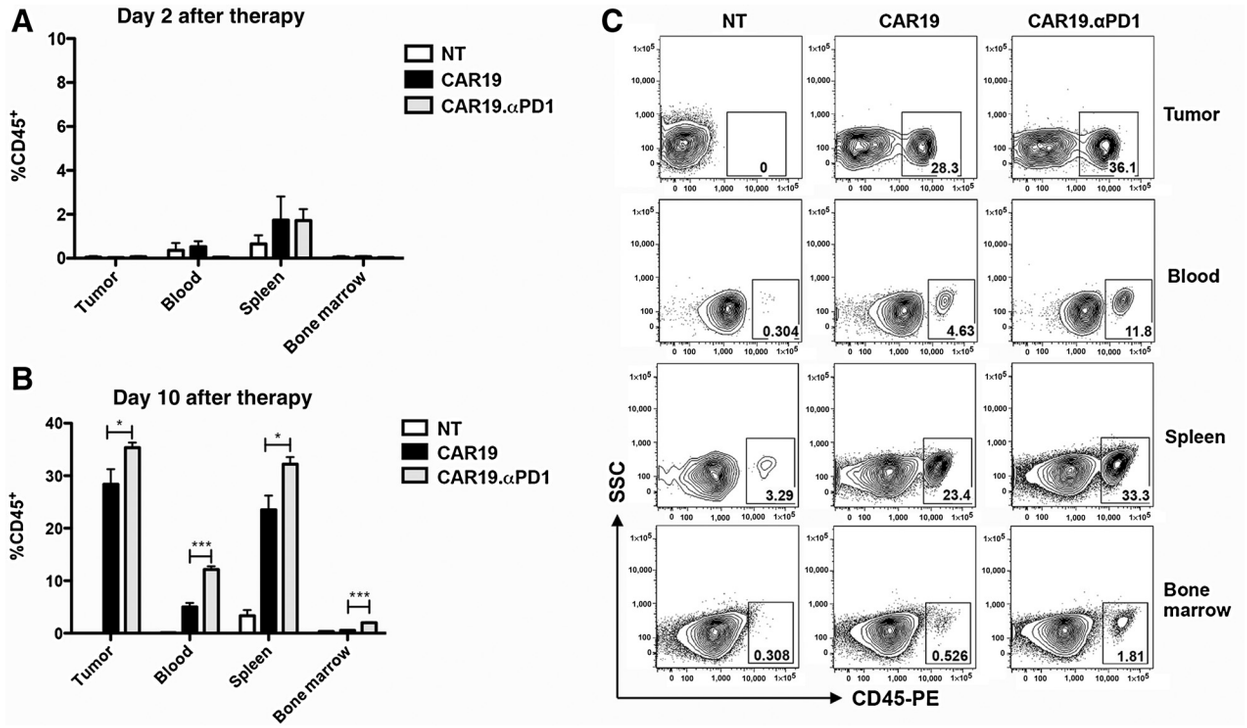

Figure 5.

CAR T cells secreting anti–PD-1 were expanded more efficiently than parental CAR T cells *in vivo*. The percentage of human CD45$^+$ T cells in the tumor, blood, spleen, and bone marrow of H292-CD19 tumor-bearing mice that were adoptively transferred with nontransduced (NT), CAR19, or CAR19.αPD1 T cells was investigated by flow cytometry at day 2 (**A**) or day 10 (**B**) after therapy ($n = 3$, mean ± SEM; *, $P < 0.05$; ***, $P < 0.001$). **C,** A representative FACS scatter plot of the percentage of human CD45$^+$ T cells in the tumor, blood, spleen, and bone marrow of different groups.

CAR19.αPD1 T cells, when compared with parental CAR19 T cells, further enhanced antitumor activity and prolonged overall survival. Mechanistically, we observed that CAR19.αPD1 T cells had greater *in vivo* expansion. In addition, at the local tumor site, CAR19.αPD1 T cells were shown to be less exhausted and more functional than parental CAR19 T cells.

The engagement of PD-1 and its ligand PD-L1 or PD-L2 transduces an inhibitory signal and suppresses T-cell function in the presence of TCR or BCR activation (24–26). In this study, the presence of recombinant human PD-L1 protein (rhPD-L1) significantly inhibited T-cell activation in an *in vitro* activation assay. To examine the binding and blocking activity of anti-PD-1 scFv secreted by CAR19.αPD1 T cells, we cultured the T cells with cell culture supernatant from either CAR19 T cells or CAR19.αPD-1 T cells in the presence of rhPD-L1 protein. We observed that the supernatant from CAR19.αPD1 T cells rescued T-cell function and significantly increased IFNγ production, indicating that secreted anti–PD-1 could successfully bind to PD-1 and reverse the inhibitory effects of the PD-1/PD-L1 interaction on T-cell function.

The PD-1/PD-L1 pathway involves the regulation of cytokine production by T cells, inhibiting production of IFNγ, TNFα, and IL2 (24). PD-1 expression of human GD2 and anti-HER2 CAR T cells has been shown to increase following antigen-specific activation, and PD-1 blockade has been shown to enhance T-cell effector function and increase the production of IFNγ in the presence of PD-L1$^+$ target cells (22, 27). Therefore, in this study, to compare the functional capacity of CAR19 T and CAR19.αPD1 T cells, we cocultured T cells with a PD-L1$^+$ cancer cell line, H292-CD19 or SKOV3-CD19, and found that the anti–PD-1–secreting CAR19 T cells produced a significantly higher level of IFNγ than parental CAR19 T cells. In addition to cytokine production, PD-1 can also inhibit T-cell proliferation (28). With CAR-specific stimulation in the presence of PD-L1$^+$ cancer cells, we found that CAR19.αPD1 T cells had a significantly higher proliferation potential than the parental CAR19 T cells. Taken together, these data imply that PD-1/PD-L1 signaling blockade results in more functional CAR19.αPD1 T cells with higher proliferation capacity compared with CAR19 T cells alone.

To better understand how secreted anti–PD-1 affects the function of CAR19.αPD1 T cells, we exposed CAR19 T cells and CAR19.αPD1 T cells to PD-L1$^+$ target cells and examined the expression of T-cell–inhibitory markers, including PD-1, LAG-3, and TIM-3. We observed significantly lower PD-1 expression on CAR19.αPD1 T cells, as well as lower expression of other inhibitory markers, such as LAG-3, compared with parental CAR19 T cells. The decreased expression of PD-1 in CAR19.αPD1 T cells is caused by the dual effects of antibody blockade and downregulation of PD-1 surface expression (22, 27). PD-1 upregulation on tumor-infiltrating T cells was reported to be a major contributor to T cell hypofunction in high PD-L1–expressing tumors. Downregulation of PD-1 may contribute to reversion of T-cell hypofunction and enhanced T-cell effector function, which is supported by increased IFNγ production of CAR19.αPD1 T cells. In addition, the lower expression level of other inhibitory makers, such as LAG-3, may also contribute to the higher function of CAR19.αPD1 T cells upon antigen stimulation. Our observation

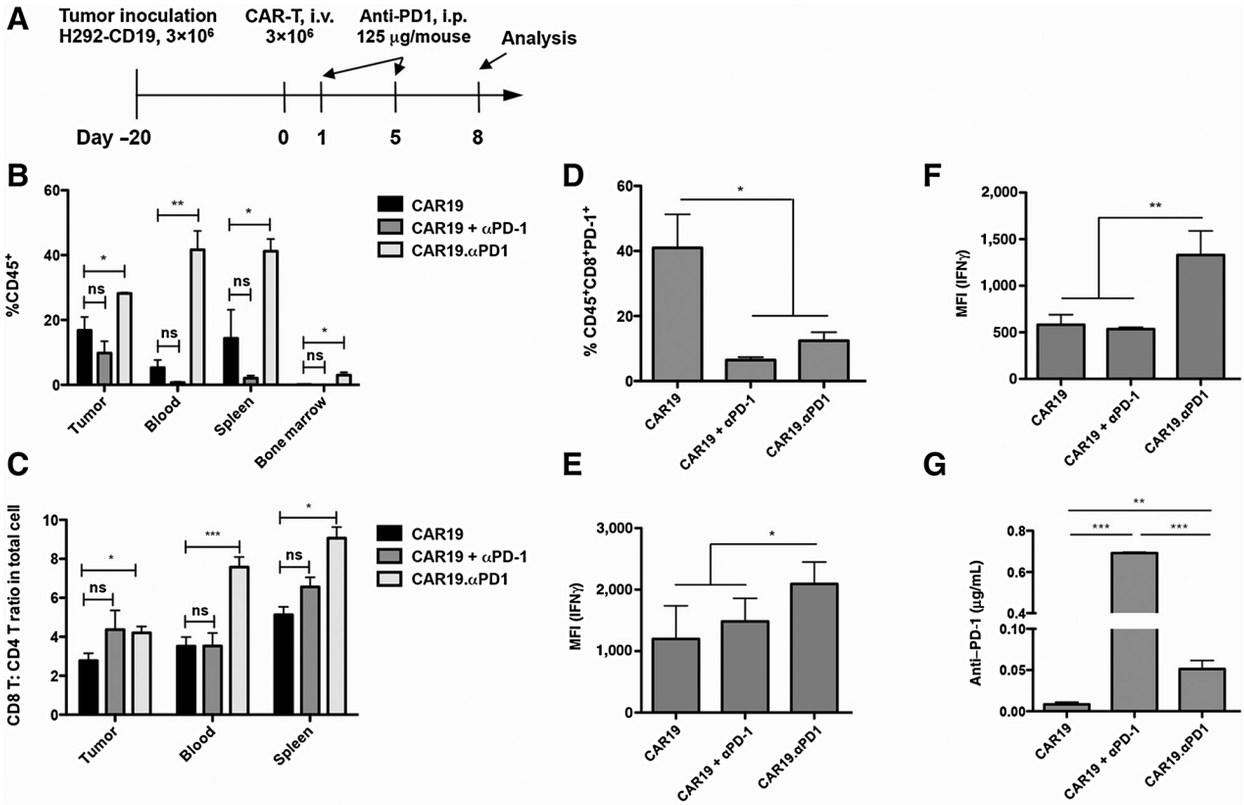

Figure 6.

CAR T cells secreting anti–PD-1 were more functional than parental CAR T cells at local tumor site. **A,** Schematic representation of the experimental procedure for tumor challenge, T-cell adoptive transfer, and antibody treatment. NSG mice were subcutaneously challenged with 3×10^6 of H292-CD19 tumor cells. At day 20, 3×10^6 of CAR19 or CAR19.αPD1 T cells were adoptively transferred through intravenous injection. One day after T-cell adoptive transfer, anti–PD-1 antibody treatment was initiated, and the treatment was continued on the indicated dates. The mice were then euthanized on day 8 for analysis. **B,** The percentage of human $CD45^+$ T cells in the tumor, blood, spleen, and bone marrow of H292-CD19 tumor-bearing mice that were adoptively transferred with CAR19 or CAR19.αPD1 T cells, or treated with CAR19 T cells along with injection of anti–PD-1 antibody, was investigated by flow cytometry (ns, not significant, $P > 0.05$; *, $P < 0.05$; **, $P < 0.01$). **C,** The ratio of $CD8^+$ versus $CD4^+$ T cells in the tumor, blood, and spleen ($n = 3$, mean ± SEM; ns, not significant, $P > 0.05$; *, $P < 0.05$; ***, $P < 0.001$). **D,** The percentage of PD-1–expressing CD8 TILs over total $CD8^+$ TILs ($n = 3$, mean ± SEM; *, $P < 0.05$). TILs were harvested and stimulated *ex vivo* for 6 hours by either anti-CD3/anti-CD28 antibodies (**E**) or target cells H292-CD19 (**F**). The percentage of CAR T cells in the tumor expressing intracellular IFNγ was investigated by flow cytometry ($n = 3$, mean ± SEM; *, $P < 0.05$; **, $P < 0.01$). **G,** The secreted anti–PD-1 scFvs and injected anti–PD-1 antibodies in the sera were evaluated using ELISA ($n = 3$, mean ± SEM; **, $P < 0.01$; ***, $P < 0.001$).

is consistent with a recent study, demonstrating that coexpression of multiple inhibitory receptors is a cardinal feature of T-cell exhaustion (29, 30). Moreover, we found that PD-L1 expression was significantly increased on CAR T cells with antigen-specific stimulation, which may also contribute to T-cell hypofunction through T cell–T cell interaction. Notably, in comparison, we observed that the expression level of PD-L1 on CAR19.αPD1 T cells was significantly lower. These data suggest that the inhibited upregulation of PD-1 and PD-L1 expression on CAR19.αPD1 T cells may contribute to the reduction of tumor cell–induced and/or T cell–induced inhibitory signaling, thereby further enhancing T-cell effector function and its antitumor immunity.

Our *in vivo* study showed that the tumor growth could be inhibited by CAR T-cell treatment, irrespective of PD-1/PD-L1 blockade. Compared with CAR19 T-cell treatment or combined CAR19 T-cell and systemic anti–PD-1 antibody treatment, in which 67% of the mice still had either stable or progressive disease, we observed that CAR19.αPD1 T-cell treatment achieved more than 90% tumor eradication in about 2 weeks. To understand the underlying mechanism of enhanced antitumor efficacy of CAR19.αPD1 T cells, we analyzed the expansion of adoptively transferred T cells *in vivo*. Consistent with our *in vitro* data, we found that the anti–PD-1–secreting CAR T cells were expanded significantly more than parental CAR T cells in all examined tissues, including tumor, blood, spleen, and bone marrow. Moreover, the population of cytotoxic $CD8^+$ T cells among TILs is critical in eliciting antitumor immunity (23). A previous study demonstrated that PD-1 signaling is involved in regulating the expansion and function of $CD8^+$ TILs (31). In this study, the larger population of $CD8^+$ TILs expresses IFNγ when stimulated *ex vivo* and the higher ratio of $CD8^+$ versus $CD4^+$ TILs in the CAR19.α PD1 T-cell group implies that CAR19.αPD1 T cells are more functional and expandable *in vivo* compared with parental CAR19 T cells.

Our data show that for the CAR19.αPD1 T-cell group, the ratio of $CD8^+$ versus $CD4^+$ T cells was significantly lower in tumor than that in blood and spleen (Supplementary Fig. S7B). Carter and colleagues reported that $CD8^+$ T cells are more sensitive to

PD-1–mediated inhibition than $CD4^+$ T cells (32). In tumor microenvironment, which is enriched by the $PD\text{-}L1^+$ tumor cells, even with the secretion of anti–PD-1 antibody, $CD8^+$ T cells remain more likely to be inhibited than those in blood or spleen, thereby causing lower ratio of $CD8^+$ versus $CD4^+$ T cells. In addition, the active recruitment of $CD4^+$ T cells, especially Treg cells by the tumor, which has been shown by Schabowsky and colleagues may also contribute to the lower $CD8^+$ versus $CD4^+$ T cell ratio (33).

Interestingly, in this study, we demonstrated that systemic anti–PD-1 antibody injection has little effect on enhancing the antitumor efficacy of CAR T-cell therapy. In a syngeneic $HER2^+$ self-antigen tumor model, recent studies have demonstrated that a high-dosage (250 μg/mouse of anti–PD-1 antibody) PD-1 blockade was capable of enhancing the antitumor activity of anti-HER2 CAR T cells in the treatment of breast cancer (27). However, a lower dosage (200 μg/mouse) of anti–PD-1 antibody showed a limited effect on CAR T-cell therapy (34). In the current xenograft tumor model that is treated with a low dose (125 μg/mouse) of anti–PD-1, the antibody failed to inhibit tumor growth or enhance the antitumor efficacy of CAR T cells even though the amount of circulating antibody (~0.7 μg/mL) was 15-fold higher than the amount detected in the CAR19.αPD1 T-cell treatment group. This observation indicates that administration of a modest dose PD-1 antibody blockade may not be sufficient to improve the therapeutic outcome of CAR T-cell therapy. Although both administered and self-secreting anti–PD-1 antibodies efficiently decreased and blocked the PD-1 expression in $CD8^+$ T cells *in vivo*, systemically injected anti–PD-1 antibody had little effect on increasing the population of cytolytic $CD8^+$ TILs or enhancing IFNγ production of TILs upon *ex vivo* stimulation. This result suggests that the injected antibody has little effect on augmenting infused T-cell function at the current dose, which may contribute to the observed failure of injected PD-1 blockade in enhancing the antitumor activity of CAR T-cell therapy. Indeed, according to our combination treatment regime, the PD-1 antibody was administered 24 hours after CAR T-cell infusion, and one may argue that this delay may have also been a contributing factor to the subpar effect on enhancing the antitumor efficacy of CAR T cells. However, our *in vivo* results demonstrated that CAR T-cell homing to the tumor is low within the first 48 hours, which suggest that the delay of PD-1 antibody injection may not be a substantial factor limiting the efficacy of the combination treatment. Thus, given the low concentration of secreted anti–PD-1 and the augmented effector function at the local tumor tissue, the anti–PD-1 secreted by CAR T cells may provide a safer and more potent approach in blocking PD-1 signaling and enhancing the functional capacity of CAR T cells.

In conclusion, CAR19.αPD1 T cells exhibited alleviated T-cell hypofunction, enhanced T-cell expansion, and improved CAR T-cell treatment of human solid tumors in a xenograft mouse model. It is worth noting that other than PD-1, the self-secreting anti–PD-1 has little effect on the other examined T-cell–inhibitory markers, such as LAG-3 and TIM-3. Given that PD-1 is one of major effector molecules in mediating T-cell exhaustion (35), further studies are needed to evaluate whether the self-secreting anti–PD-1 has a role in ameliorating T-cell exhaustion. In this study, even though CD19 may not be an ideal antigen for the study of solid tumors, our data indeed imply that self-secreting anti–PD-1 CAR T cells could be another promising approach to improve the capacity of CAR T-cell therapy in the treatment of solid tumors. For future studies, other solid tumor antigens, such as mesothelin or HER2, should be investigated to better evaluate the antitumor efficacy of CAR.αPD1 T cells for solid tumors. In addition, it is unclear from our current study how the self-secreted anti-PD-1 affects immune cells other than infused CAR T cells in tumor. Given the durable effect of PD-1 blockade on modulating the tumor microenvironment (12, 36), it could be beneficial to explore the capacity of CAR.αPD1 T cells to eradicate solid tumor in an immunocompetent condition, such as syngeneic mouse models. We anticipate that in such a condition, anti–PD-1–engineered CAR T cells may be more effective in inducing tumor eradication.

Disclosure of Potential Conflicts of Interest

P. Wang is a consultant/advisory board member for HRAIN Biotechnology. No potential conflicts of interest were disclosed by the other authors.

Authors' Contributions

Conception and design: S. Li, N. Siriwon, F. He, S. Wang, P. Wang
Development of methodology: S. Li, N. Siriwon, S. Yang, T. Jin, F. He
Acquisition of data (provided animals, acquired and managed patients, provided facilities, etc.): S. Li, N. Siriwon, X. Zhang, S. Yang, F. He, Y.J. Kim, J. Mac, X. Han
Analysis and interpretation of data (e.g., statistical analysis, biostatistics, computational analysis): S. Li, N. Siriwon, F. He, Z. Lu, P. Wang
Writing, review, and/or revision of the manuscript: S. Li, N. Siriwon, F. He, J. Mac, Z. Lu, P. Wang
Administrative, technical, or material support (i.e., reporting or organizing data, constructing databases): S. Li, N. Siriwon, T. Jin, F. He, S. Wang, P. Wang
Study supervision: T. Jin, P. Wang

Acknowledgments

The authors thank the University of Southern California Flow Cytometry Core for the assistance.

Grant Support

This work was supported by NIH grants (R01AI068978, R01CA170820, R01EB017206, and P01CA132681) and a translational acceleration grant from the Joint Center for Translational Medicine (to P. Wang).

The costs of publication of this article were defrayed in part by the payment of page charges. This article must therefore be hereby marked *advertisement* in accordance with 18 U.S.C. Section 1734 solely to indicate this fact.

Received March 24, 2017; revised July 9, 2017; accepted September 8, 2017; published OnlineFirst September 14, 2017.

References

1. Grupp SA, Kalos M, Barrett D, Aplenc R, Porter DL, Rheingold SR, et al. Chimeric antigen receptor-modified T cells for acute lymphoid leukemia. N Engl J Med 2013;368:1509–18.
2. Khammari A, Labarriere N, Vignard V, Nguyen JM, Pandolfino MC, Knol AC, et al. Treatment of metastatic melanoma with autologous melan-A/mart-1-specific cytotoxic T lymphocyte clones. J Invest Dermatol 2009;129:2835–42.
3. Mackensen A, Meidenbauer N, Vogl S, Laumer M, Berger J, Andreesen R. Phase I study of adoptive T-cell therapy using antigen-specific CD8(+) T cells for the treatment of patients with metastatic melanoma. J Clin Oncol 2006;24:5060–9.
4. Maus MV, Grupp SA, Porter DL, June CH. Antibody-modified T cells: CARs take the front seat for hematologic malignancies. Blood 2014;123:2625–35.

5. Park JH, Geyer MB, Brentjens RJ. CD19-targeted CAR T-cell therapeutics for hematologic malignancies: interpreting clinical outcomes to date. Blood 2016;127:3312–20.
6. Davila ML, Riviere I, Wang X, Bartido S, Park J, Curran K, et al. Efficacy and toxicity management of 19-28z CAR T cell therapy in B cell acute lymphoblastic leukemia. Sci Transl Med 2014;6:224ra25.
7. Louis CU, Savoldo B, Dotti G, Pule M, Yvon E, Myers GD, et al. Antitumor activity and long-term fate of chimeric antigen receptor-positive T cells in patients with neuroblastoma. Blood 2011;118:6050–6.
8. Gui L, Han XH, He XH, Song YY, Yao JR, Yang JL, et al. Phase I study of chimeric anti-CD20 monoclonal antibody in Chinese patients with CD20-positive non-Hodgkin's lymphoma. Chin J Cancer Res 2016;28: 197–208.
9. Kershaw MH, Westwood JA, Darcy PK. Gene-engineered T cells for cancer therapy. Nat Rev Cancer 2013;13:525–41.
10. Bonifant CL, Jackson HJ, Brentjens RJ, Curran KJ. Toxicity and management in CAR T-cell therapy. Mol Ther Oncolytics 2016;3:16011.
11. Gill S, Maus MV, Porter DL. Chimeric antigen receptor T cell therapy: 25years in the making. Blood Rev 2016;30:157–67.
12. Pardoll DM. The blockade of immune checkpoints in cancer immunotherapy. Nat Rev Cancer 2012;12:252–64.
13. Yamazaki T, Akiba H, Iwai H, Matsuda H, Aoki M, Tanno Y, et al. Expression of programmed death 1 ligands by murine T cells and APC. J Immunol 2002;169:5538–45.
14. Brown JA, Dorfman DM, Ma FR, Sullivan EL, Munoz O, Wood CR, et al. Blockade of programmed death-1 ligands on dendritic cells enhances T cell activation and cytokine production. J Immunol 2003;170:1257–66.
15. Dong HD, Strome SE, Salomao DR, Tamura H, Hirano F, Flies DB, et al. Tumor-associated B7-H1 promotes T-cell apoptosis: a potential mechanism of immune evasion. Nat Med 2002;8:793–800.
16. Konishi J, Yamazaki K, Azuma M, Kinoshita I, Dosaka-Akita H, Nishimura M. B7-h1 expression on non-small cell lung cancer cells and its relationship with tumor-infiltrating lymphocytes and their PD-1 expression. Clin Cancer Res 2004;10:5094–100.
17. Moon EK, Wang LC, Dolfi DV, Wilson CB, Ranganathan R, Sun J, et al. Multifactorial T-cell hypofunction that is reversible can limit the efficacy of chimeric antigen receptor-transduced human T cells in solid tumors. Clin Cancer Res 2014;20:4262–73.
18. Chong EA, Melenhorst JJ, Lacey SF, Ambrose DE, Gonzalez V, Levine BL, et al. PD-1 blockade modulates chimeric antigen receptor (CAR)-modified T cells: refueling the CAR. Blood 2017;129:1039–41.
19. Han X, Bryson PD, Zhao Y, Cinay GE, Li S, Guo Y, et al. Masked chimeric antigen receptor for tumor-specific activation. Mol Ther 2017;25:274–84.
20. Engels B, Cam H, Schuler T, Indraccolo S, Gladow M, Baum C, et al. Retroviral vectors for high-level transgene expression in T lymphocytes. Hum Gene Ther 2003;14:1155–68.
21. Wang C, Thudium KB, Han M, Wang XT, Huang H, Feingersh D, et al. In vitro characterization of the anti-PD-1 antibody Nivolumab, BMS-936558, and in vivo toxicology in non-human primates. Cancer Immunol Res 2014;2:846–56.
22. Gargett T, Yu WB, Dotti G, Yvon ES, Christo SN, Hayball JD, et al. GD2-specific CAR T cells undergo potent activation and deletion following antigen encounter but can be protected from activation-induced cell death by PD-1 blockade. Mol Ther 2016;24:1135–49.
23. Hadrup S, Donia M, Thor Straten P. Effector CD4 and CD8 T cells and their role in the tumor microenvironment. Cancer Microenviron 2013;6: 123–33.
24. Riella LV, Paterson AM, Sharpe AH, Chandraker A. Role of the PD-1 pathway in the immune response. Am J Transplant 2012;12:2575–87.
25. Chemnitz JM, Parry RV, Nichols KE, June CH, Riley JL. SHP-1 and SHP-2 associate with immunoreceptor tyrosine-based switch motif of programmed death 1 upon primary human T cell stimulation, but only receptor ligation prevents T cell activation. J Immunol 2004;173: 945–54.
26. Koyama S, Akbay EA, Li YY, Herter-Sprie GS, Buczkowski KA, Richards WG, et al. Adaptive resistance to therapeutic PD-1 blockade is associated with upregulation of alternative immune checkpoints. Nat Commun 2016; 7:10501.
27. John LB, Devaud C, Duong CPM, Yong CS, Beavis PA, Haynes NM, et al. Anti-PD-1 antibody therapy potently enhances the eradication of established tumors by gene-modified T cells. Clin Cancer Res 2013;19: 5636–46.
28. Keir ME, Butte MJ, Freeman GJ, Sharpe AH. PD-1 and its ligands in tolerance and immunity. Annu Rev Immunol 2008;26:677–704.
29. Wherry EJ, Kurachi M. Molecular and cellular insights into T cell exhaustion. Nat Rev Immunol 2015;15:486–99.
30. Thommen DS, Schreiner J, Muller P, Herzig P, Roller A, Belousov A, et al. Progression of lung cancer is associated with increased dysfunction of T cells defined by coexpression of multiple inhibitory receptors. Cancer Immunol Res 2015;3:1344–55.
31. Chauvin J-M, Pagliano O, Fourcade J, Sun Z, Wang H, Sander C, et al. TIGIT and PD-1 impair tumor antigen-specific $CD8^+$ T cells in melanoma patients. J Clin Invest 2015;125:2046–58.
32. Carter L, Fouser LA, Jussif J, Fitz L, Deng B, Wood CR, et al. PD-1:PD-L inhibitory pathway affects both CD4(+) and CD8(+) T cells and is overcome by IL-2. Eur J Immunol 2002;32:634–43.
33. Schabowsky RH, Madireddi S, Sharma R, Yolcu ES, Shirwan H. Targeting CD4+CD25+FoxP3+ regulatory T-cells for the augmentation of cancer immunotherapy. Curr Opin Investig Drugs 2007;8:1002–8.
34. Beavis PA, Henderson MA, Giuffrida L, Mills JK, Sek K, Cross RS, et al. Targeting the adenosine 2A receptor enhances chimeric antigen receptor T cell efficacy. J Clin Invest 2017;127:929–41.
35. Lee J, Ahn E, Kissick HT, Ahmed R. Reinvigorating exhausted T cells by blockade of the PD-1 pathway. For Immunopathol Dis Ther 2015;6:7–17.
36. Santarpia M, Karachaliou N. Tumor immune microenvironment characterization and response to anti-PD-1 therapy. Cancer Biol Med 2015; 12:74–8.